J. Fluid Mech. (1988), *vol.* 187, *pp.* 451–466
Printed in Great Britain

Measurements of the mean force on a particle near a boundary in turbulent flow

By D. HALL
CEGB Berkeley Nuclear Laboratories, Berkeley, Gloucestershire GL13 9PB, UK

(Received 22 December 1986 and in revised form 4 September 1987)

The transport of particles through gaseous systems is controlled by three factors: their arrival to the surface; whether or not they bounce upon impact; and when (if ever) they are resuspended from the surface. One of the parameters required in determining whether or not a particle is suspended is the lift force acting on the particle. We demonstrate that the fluid lift forces acting on particles as small as 1 μm in diameter can be modelled by particles of several mm in diameter. However, the forces involved in modelling such small particles are around 10^{-8} N, which is several orders of magnitude smaller than reported in published measurements of fluid lift forces. A system to determine such lift forces has been developed and is described. Measurements of the mean force acting on particles on both rough and smooth surfaces are presented.

The data recorded here for the mean fluid lift force on a sphere on a smooth surface are in good agreement with the relationship

$$F^+ = (20.90 \pm 1.57)(a^+)^{2.31 \pm 0.02},$$

where F^+ is the non-dimensional force and a^+ the non-dimensional particle radius scaled on fluid-boundary-layer parameters. It was observed that surface roughness can change the force by up to a factor of six.

1. Introduction

Many situations exist in which a greater understanding of the mechanisms causing the removal of particles by fluid flows could usefully be applied. The cleaning of surfaces by water jets and vacuum cleaners, and the contamination of surfaces due to the suspension and subsequent deposition of materials are obvious examples. In the Nuclear Industry we are interested in the transport of particles both in nuclear-reactor coolant circuits and in the disposal route for irradiated fuel.

The transport of particles through a gas system is controlled by three factors:

(i) the arrival rate of particles to a surface;

(ii) whether or not the particles bounce on impact with the surface; and

(iii) whether or not the particles are resuspended from the surface.

Reeks, Reed & Hall (1987) have developed a model of particle transport in which the resuspension rates of particles from a surface plays a major role. One of the parameters required by the model is the fluid lift force acting on a particle on a surface.

Several authors have estimated the lift forces on spheres by obtaining approximate solutions to the equations of motion of a fluid around a sphere. O'Neill (1968) derived a solution for the forces acting on a sphere upon a surface by assuming that only

viscous effects contributed to the forces experienced by the particle, effects due to the inertia of the fluid being neglected. He concluded that, in this case, there was no force normal to the direction of flow. This agrees with the general conclusion reached by Bretherton (1962) that no sideways force on a single, rigid, spherical particle can be derived on the basis of the creeping-flow equation whatever the velocity profile and relative size of particle and tube, provided, of course, that the velocity is unidirectional.

Saffman (1965) considered the case of a sphere in a shear flow under conditions where the particle Reynolds numbers based upon mean fluid velocity, the shear gradient and the angular velocity of the particle, were all much less than one. By including first-order effects due to the fluid inertia he derived an expression for the force acting upon the sphere in a direction normal to the fluid flow. However, this solution is only valid for a particle in the body of a fluid and, as noted by Saffman, would not be expected to hold for a sphere on, or near to, a surface.

Leighton & Acrivos (1985) extended O'Neill's analysis to include first-order effects of inertia in a similar manner to Saffman. However, their solution is only strictly valid when the shear Reynolds number is much less than one, and is therefore of limited applicability.

Goren (1970) produced a solution for the force, normal to the surface, acting upon a particle on a surface in a stagnation flow field. He considered the case of creeping flow only, as did O'Neill; however in Goren's case the flow direction was normal to the surface.

Cleaver & Yates (1973) used Goren's relationship to estimate the lift force on a particle in a turbulent boundary layer by matching the stagnation flows to the observed fluctuations in the sublayer flow. They compared the predictions given by this approach with the results given by assuming that Saffman's relationship could be applied to a particle on a surface, and found that the second approach predicted forces over two orders of magnitude greater than predicted by use of Goren's theory.

All these theories are unproven and they cannot be extrapolated to situations where larger particle Reynolds numbers are encountered. (In nuclear reactors we are particularly concerned with particles between 1 and 100 μm in diameter. Such deposited particles have Reynolds numbers in the range 1–1000.) In the absence of suitable theoretically based methods, experimental methods have to be used to evaluate the fluid-induced forces acting to remove a particle from a surface.

Direct measurement of the fluid lift force acting on a particle of several microns in size would present considerable, if not insurmountable, technical difficulties, hence a method of modelling such situations is required. Provided that the fluid can be treated as a continuum (i.e. its mean free path is much less than the particle diameter) then the only fundamental parameters of importance in determining the force on a sphere of radius a on a surface in a fully developed turbulent boundary-layer flow are the density ρ, viscosity μ and friction velocity u_τ of the fluid. If we take unit distance as $\rho\mu/u_\tau$, unit mass as $\mu^3/\rho u_\tau^3$ and unit time as $\mu/u_\tau^2\rho$, then the mean fluid induced forces acting on a sphere can be described by the parameters

$$F^+ = F/\nu^2\rho, \quad a^+ = \frac{au_\tau}{\nu},$$

where $\nu(=\mu/\rho)$ is the kinematic viscosity. Hence we can use relatively large particles to determine the forces on the small particles of interest. For example, a 10 μm

diameter particle in the core of an Advanced Gas Cooled Reactor can be modelled using a 1 mm diameter ball in an air flow of 1.6 m s^{-1} at atmospheric pressure.

Willetts & Murray (1981) reviewed and reported direct measurements of the fluid-induced lift forces acting on spheres at, or close to, a surface. In all cases quoted the particle Reynolds number, based on the mean velocity of the fluid past the sphere, was greater than, or equal to, 800. However, there are many practical cases, such as the reactor circuit, where particle Reynolds numbers are orders of magnitude less than this while still being too large to allow the use of creeping-flow solutions.

The experimental approaches quoted by Willetts & Murray are generally unsuitable where particle Reynolds numbers are less than a few hundred. There are two basic problems:

(i) the force resolution of the systems described by Willetts & Murray were at best about 10^{-4} N; ideally a resolution of 10^{-8} to 10^{-9} N is required to cover the lower particle Reynolds numbers;

(ii) the apparatus used billiard-ball-sized particles ($\sim$ 40 mm diameter) on which to monitor forces; to model the forces on such a particle in the boundary layer of a turbulent fluid would require very large flow channels. Ideally, the particles need to be a few mm in diameter.

This note describes a system capable of measuring mean lift forces as low as 10^{-8} N (the weight of, say, a single grain of castor sugar). Measurements of the mean lift force acting on spheres, both on and near to smooth and rough surfaces, with non-dimensional particle radii between 1.8 and 70 (Reynolds numbers 6.5–1250) are presented and discussed. The fluctuating component of the lift force is currently being measured and will form the basis of a further paper.

2. Apparatus

An exhaustive description of the apparatus is published elsewhere (Hall 1984); accordingly, only a brief description is given here. The particle on which the force is measured is held captive by a tungsten support wire just above the floor of a wind tunnel. The transducer arrangement is shown in figure 1. The particle can be raised above the surface and it can also be tilted (to determine drag forces). The tungsten support wire passes through a narrow hole in the top surface insert and is engineered to avoid contact between the insert and the wire.

The 'heart' of the system is a Maywood Microforce transducer manufactured by Maywood Instruments, Basingstoke, Hants., England. A diagram of the force-sensing part of the transducer is shown in figure 2. As can be seen from the figure, the geometric arrangement of the transducer is such that movement of the transducer load button occurs predominantly along one direction. Four semi-conductor strain gauges form a bridge from which the amount of movement of the transducer load button can be measured and hence any force change evaluated. The output of the transducer was put through a low-pass filter to reduce its variance and so allow better determination of its mean value.

The amplified outputs from the force transducer and other transducers monitoring the fluid velocity, humidity, pressure and temperature, are recorded by a datalogger and communicated to a computer for analysis. The computer is also used to control the rig.

Forces on a sphere on both rough and smooth surfaces have been measured. Five geometries have been considered in an attempt to gain a limited understanding of the influence of substrate geometry upon the forces acting on particles on rough surfaces.

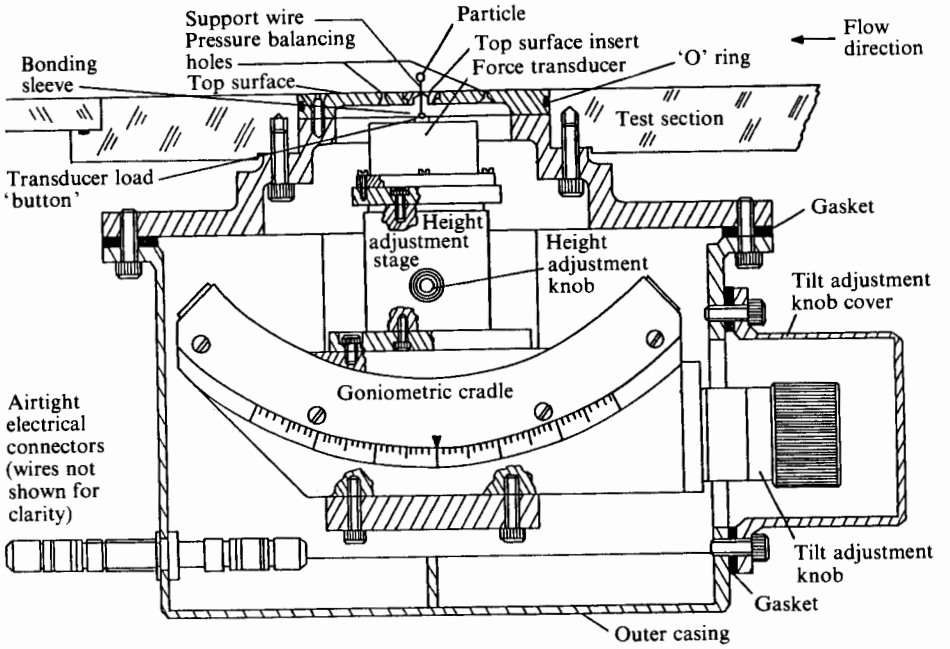

FIGURE 1. Force-transducer arrangement.

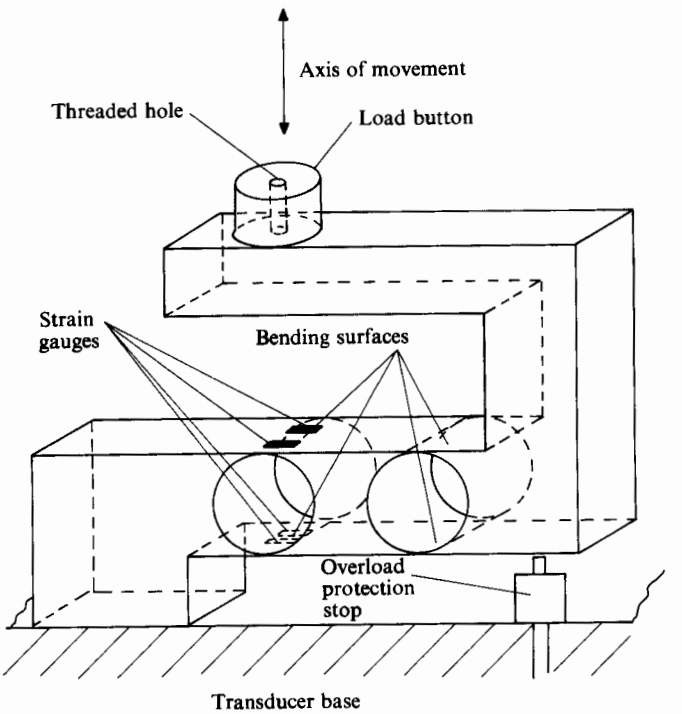

FIGURE 2. The force transducer.

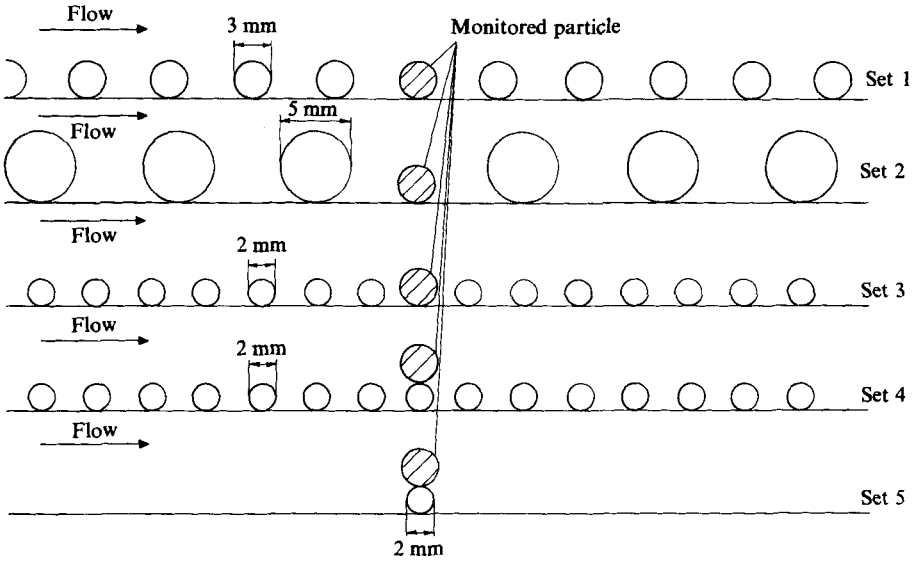

FIGURE 3. The geometry of the rods around the monitored particles for the five series of runs.

The geometries are shown in figure 3. For each geometry, or set, the force on a 3 mm diameter sphere was monitored. The roughness consisted of various arrangements of cylindrical rods placed across the flow.

In order to simulate a particle deposited in a trough, evenly spaced rods were placed upstream and downstream of the particle, extending for about 50 mm in both directions. Three sizes of rods were used: 3 mm for set 1; 5 mm for set 2; and 2 mm for set 3. In all cases the spacing between the rods was equal to their diameter.

To model a particle deposited on a roughness peak two sets of data were taken. Set 4 had the sphere on top of the rods used in set 3, and set 5 had the sphere on a single rod. The position of the test particle relative to the rods is shown, to scale, for all five geometries, in figure 3.

3. Calibration of the force measurement system

Three factors determine the response of the system: (i) force sensitivity normal to the surface; (ii) sensitivity to side loads; (iii) pressure sensitivity.

The procedure for calibration was the same as that described earlier (Hall 1984). Measurements of force sensitivity were performed by measuring the change in system output when weights were attached to the transducer. There were either placed directly on the transducer load button (see figure 1) or placed on a hook attached to the load button to allow measurements of the sensitivity to side loads (with the transducer tilted to make the force act in the desired direction). Measurements of pressure sensitivity were made by noting the response of the system to large changes in pressure.

Table 1 contains the calibration data for the two transducers used in this series of experiments.

Transducer	1	2
Force sensitivity normal to surface (V N^{-1})	0.279	1.295
Angle for zero sensitivity to force in the flow direction	7.08°	6.07°
Force sensitivity parallel to the surface and normal to flow direction as a % of the sensitivity normal to the surface	0.4%	−0.2%
Pressure sensitivity (V Pa^{-1})	$(6.2\pm1.0)\times10^{-10}$	$(2.28\pm0.04)\times10^{-9}$

TABLE 1. Calibration data

4. Procedure

The flow was set to the desired level after the temperature of the transducer had been allowed to stabilize. A Pitot-static tube was used, with a pressure transducer, to measure the flow.

The procedure used to measure F^+ and a^+ evolved through the series of experiments. Essentially a series of measurements as described in figure 4 was employed. The uncertainty in a single measurement of the change in transducer output, when force was applied, was of order of 10^{-6} N. In order to resolve forces as low as 10^{-8} N it was necessary to perform a large number of repeat measurements. In some cases as many as 10000 repeat measurements were performed.

Two methods were used to correct for the drift in the force-transducer output. Initially, the mean change in transducer output, 0, was calculated by assuming a linear drift in transducer output when flow was not applied, i.e.

$$0 = X_f - X_b + \frac{(t_f - t_b)}{(t_a - t_b)}(X_b - X_a),$$

where X_i and t_i refer to the mean output and mean times. i = f when the flow is on, i = b before the flow run and i = a after the flow run. Clearly, if the transducer output is of the form

$$A + B(t - t_b) + C(t - t_b)^2 + \ldots$$

then an error will occur due to the quadratic and higher-order terms. In order to minimize this source of error a least-squares fit was performed on the zero-flow data; two sets prior to the run with the flow on and one set after the run were used. The resulting values of the fitted coefficients (A, B and C) were used to estimate what the mean value of the transducer output would have been if flow were not applied. The mean change in output due to the flow was calculated by subtracting this value from the mean value measured with the flow on. Note that each set of measurements of the transducer output contained 70 recordings at 1 s intervals.

To ensure that the results were not affected by disturbances, such as people knocking the rig and causing the filters to overload, the computer printed out all readings when the value of F^+ was more than 4 standard deviations from the expected mean (determined by a series of trial runs). This enabled disturbances to be edited out. Finally, when the series of runs had been completed, the chi-squared test was used to ensure that the results were normally distributed.

With the exception of the friction velocity and the dynamic viscosity of the fluid, the fluid parameters were calculated in accordance with BS1042 Pt. 2A (1973). The

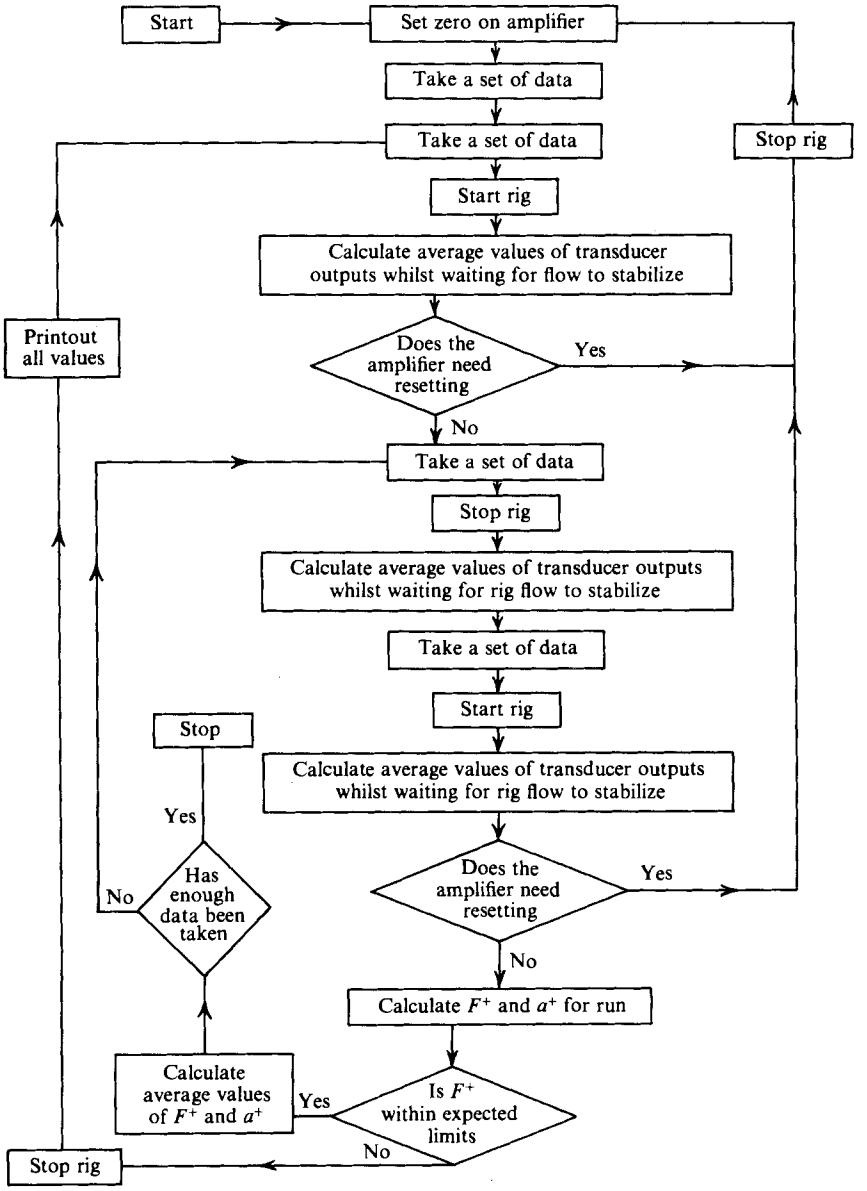

FIGURE 4. The procedure for measuring average values of F^+ and a^+.

dynamic viscosity of air was calculated using Hilsenrath *et al.*'s relationship quoted by Pirie (1978):

$$\mu = \frac{\theta^{1.5} \times 1.458 \times 10^{-6}}{(\theta + 110.4)} \text{kg m}^{-1}\text{ s}^{-1},$$

where θ is the temperature of the air in K.

The values of the friction velocity were derived by fitting the fluid velocity measured using the Pitot-static tube to the velocity profile for an aerodynamically smooth surface given by Kay & Nedderman (1974). Note that the Pitot tube was located upstream of the rough surfaces and hence the roughness would not have an effect on the Pitot-static-tube output.

5. Results

The results fall into four main categories:

(i) a series of test runs to check the performance of the system;

(ii) measurements of the variation of F^+ with height above a smooth surface;

(iii) measurements of the variation of F^+ with a^+ for a particle on a smooth surface;

(iv) measurements of the effects of surface roughness upon F^+.

The results of each of these four categories of measurements are presented and discussed in the following sections.

5.1. *Test runs*

The test runs fall into two categories: testing whether or not forces acting parallel to the surface affect the transducer output; and determining a lower limit to the resolution of the system.

A check on the effect of the drag force acting parallel to the surface was performed by comparing measurements of F^+ made with the force axis set normal to the smooth duct surface, with measurements made with the force axis tilted 1° downstream. Several sets of data were taken with the sphere set at various heights above the surface. In all cases the 1° tilt made no difference to the results. Two such sets of data, at 100 and 200 μm above the surface, are shown in figure 5. If the results obtained were due to forces acting parallel to the surface then titling the force axis by 1° would be expected to have a considerable affect on the results (as the axis was aligned to better than 0.1°). It is evident from figure 5 that this did not occur. Therefore, we can deduce that the measurements are genuine.

A summary of the test results is given in table 2. It is important to note that the axis of maximum force sensitivity of the transducer is not normal to the plane of zero sensitivity as would be the case, for example, with a simple spring. Therefore, when the test section is set level the transducer output can be affected by tilting the transducer because the component of the gravitational force acting on the moving parts of the transducer and its attachments changes. As expected, the transducer output varies as the cosine of the angle between the vertical and its angle of maximum sensitivity. It was found that maximum output occurred when the goniometric cradle was set to 2.2°, i.e. the axis of maximum force sensitivity was then aligned with gravity. As tilt sensitivity is the differential of the transducer output with tilt, the sensitivity to tilt will be a minimum at this setting. Therefore, if the rig tilted in the vertical plane parallel with the flow direction, altering the tilt angle to this setting should substantially reduce this effect.

The results of the tests listed in table 2 show that the average value of the data tends to zero when no flow is applied, but applying flow can give an error of order ± 100 in F^+. It is clear that this is not due to tilt in the vertical plane parallel with the flow direction, since the problem still occurred when the transducer mounting was tilted to minimize the sensitivity to tilt.

The problem may be due to differential expansion of the support of the goniometric cradle causing the transducer to be tilted in the vertical plane normal to the flow direction. A change in the temperature of only 0.02 °C is required to produce sufficient tilt to cause such effects (provided that the tilt sensitivity is the same in the plane normal to the flow direction as parallel with the flow direction). The magnitude of the change in transducer output would then be dependent on the ambient air

$\frac{u_\tau \rho}{\mu} \times 10^3$	F^+ Linear fit for drift	F^+ Quadratic fit for drift	Description
0	16 ± 15	31 ± 16	No flow
0	—	-4.5 ± 4.9	No flow
5.34 ± 0.04	-128 ± 28	-126 ± 29	
5.25 ± 0.07	121 ± 14	138 ± 15	No ball attached. Goniometric cradle angle set to 6.06°
2.79 ± 0.04	91 ± 24	88 ± 23	
3.08 ± 0.02	-46 ± 19	-35 ± 19	
5.25 ± 0.06	-140 ± 20	-143 ± 21	No ball attached. Goniometric cradle angle set to 2.2° where sensitivity to tilt along the length of the test section is a minimum.

TABLE 2. Details of test runs using transducer 2

temperature. Alternatively, the temperature of the transducer may change during the run owing to the flow of air around the transducer mounting.

Unfortunately, it was not possible to resolve which of these, or other unspecified mechanisms, caused the anomaly. Therefore, noting that the additional uncertainty is of order 100 in F^+, the uncertainty U has been increased to U', assuming the anomaly to be caused by an effectively random error, as given below.

$$U' = (U^2 + 100^2)^{\frac{1}{2}}$$

5.2. *Measurements of the variation of force with height above a smooth surface*

The variation of F^+ with the height of the sphere above the surface was examined in two ways. The variation of a^+ with F^+ with the ball at set distances above the surface, and the variation of F^+ with height at fixed values of a^+ were both investigated. The first group of measurements are shown in figure 5. The relationships between F^+ and a^+ for a 3 mm diameter sphere are shown for sphere heights of 15, 100 and 200 μm above the surface. Figures 6 and 7 show the variation of F^+ with height at a^+ of 5.2 ± 0.1 and 57.5 ± 0.4 respectively. We note that in all cases the fluid lift force decreases as the particle height increases.

5.3. *The variation of F^+ with a^+ for a particle on a smooth surface*

Measurements of the variation of F^+ with a^+ were taken with two different transducers using four different sphere diameters. The data taken with the two different transducers are displayed in figures 8 and 9, showing variation with the transducer used and sphere diameter respectively. For $a^+ > 20$ the particle was within 0.5% of its diameter from the surface, otherwise it was within 2% of its diameter. We note (from figure7) that at $a^+ = 57.5$ there is no significant difference in the force when the particle is less than 0.5% of its diameter above the surface, and a 20% reduction in force when the particle was 2% of its diameter from the surface. At $a^+ = 5.2$ (see figure 6) there is virtually no difference in force when the particle was 20% of its diameter from the surface. This suggests a gradual reduction in the sensitivity of F^+ to the relative height of the particle above the surface as a^+ decreases. Therefore, it seems reasonable to assume that the force acting on

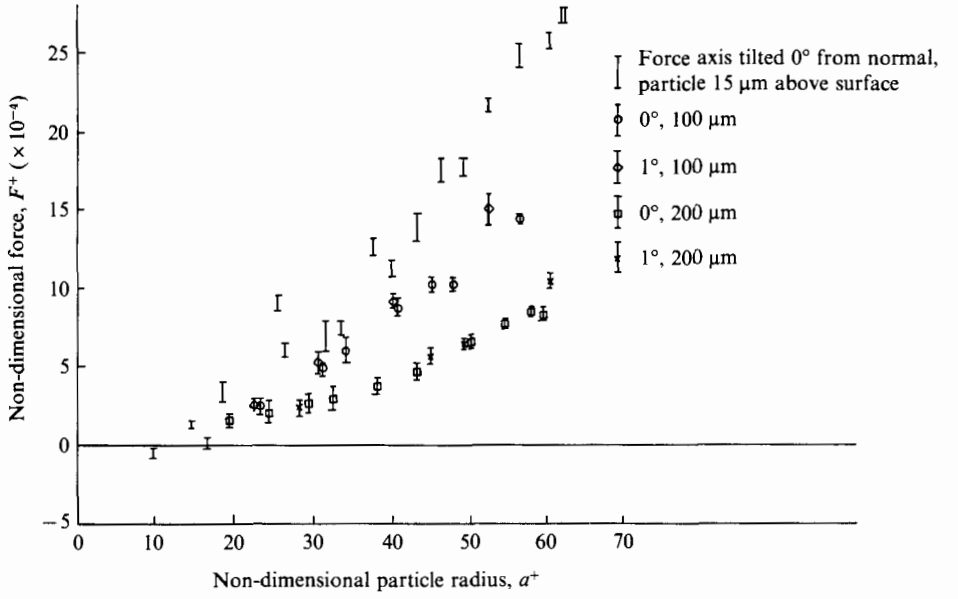

FIGURE 5. Non-dimensional force F^+ as a function of a^+ and particle height above a smooth surface for a 3 mm diameter sphere. Error bars give ± 1 standard error of estimation (68% confidence limits).

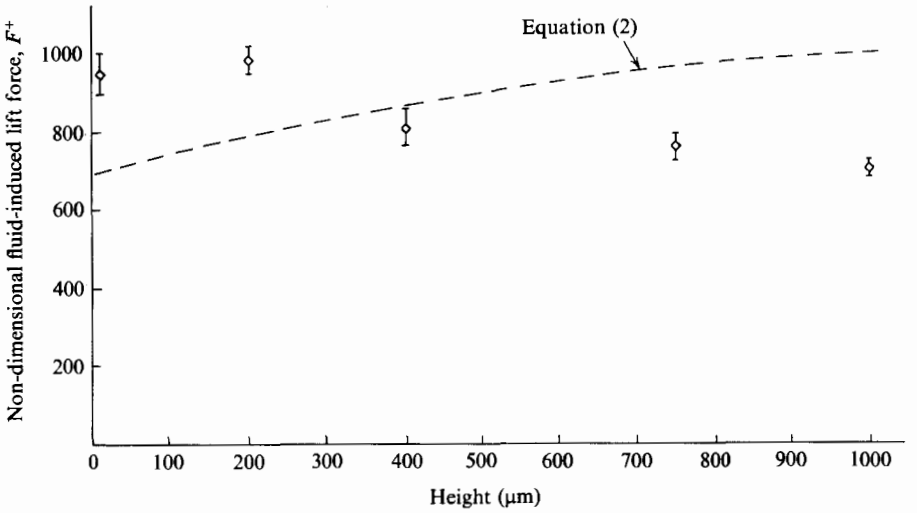

FIGURE 6. The variation of lift force with height above a smooth surface for a 1 mm diameter sphere, $a^+ = 5.2 \pm 0.1$.

the particle when its height above the surface is less than 2% of its diameter for $a^+ < 20$, and less than 0.5% of its diameter for $70 > a^+ > 20$, can be considered indistinguishable from the force acting on a particle on a surface.

In considering the validity of the data, it is encouraging to note, from figures 8 and 9, that data taken with the different transducers are in general agreement, and that the data are independent of the size of sphere used. However, there is some scatter in the data from $a^+ = 16$ to 25. Examination of the circled measurement at a^+ of

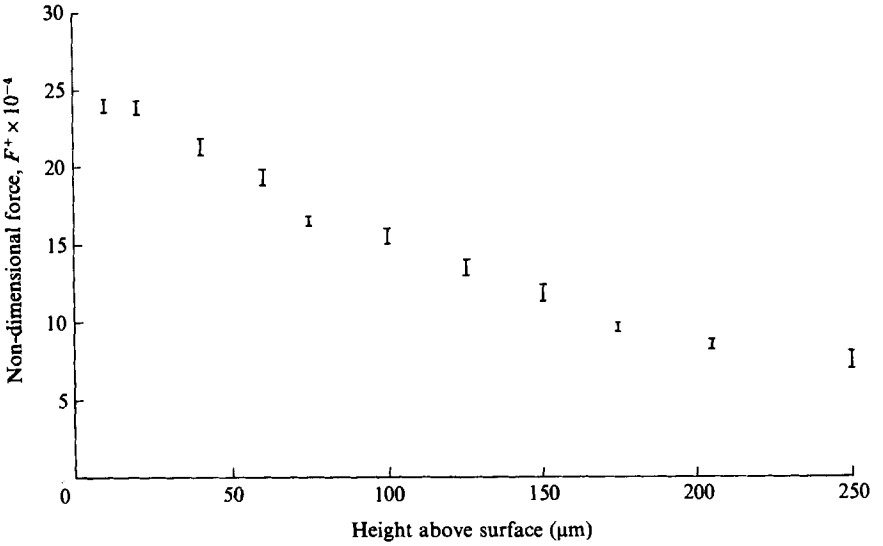

FIGURE 7. The variation of lift force with height above a smooth surface at $a^+ = 57.5 \pm 0.4$ (using a 3 mm ball). Error bars give ± 1 standard error of estimation (68% confidence limits).

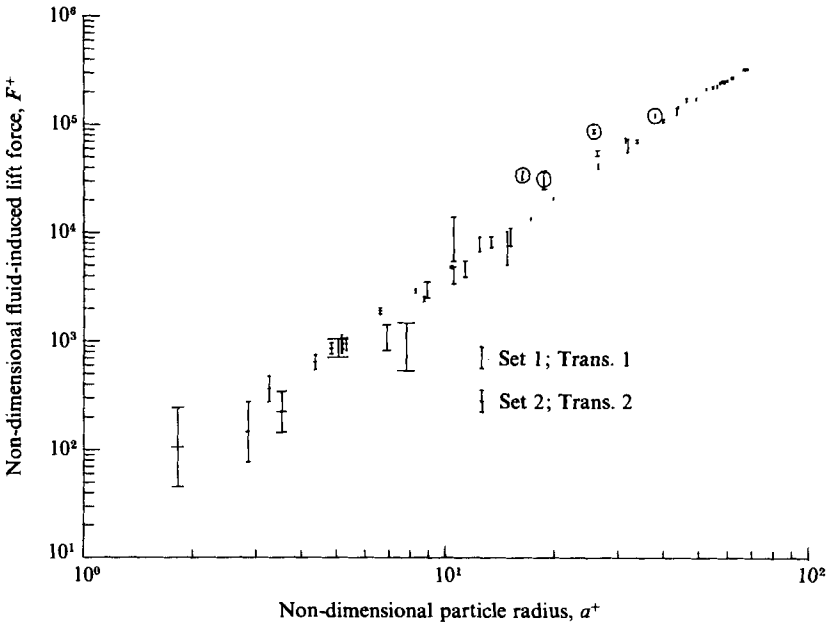

FIGURE 8. Lift force on particles on a smooth surface for two different transducers. Suspect data are circled.

about 16 (see figure 8) revealed that it was taken just after the ball had been attached to the transducer via the tungsten wire. The system had suffered from frequent problems around that time and was rebuilt before further data were taken. The three other circled points from set 1 (figure 8) all lie above the other data. They were all taken with a different amplifier from that used for the other data. It seems likely,

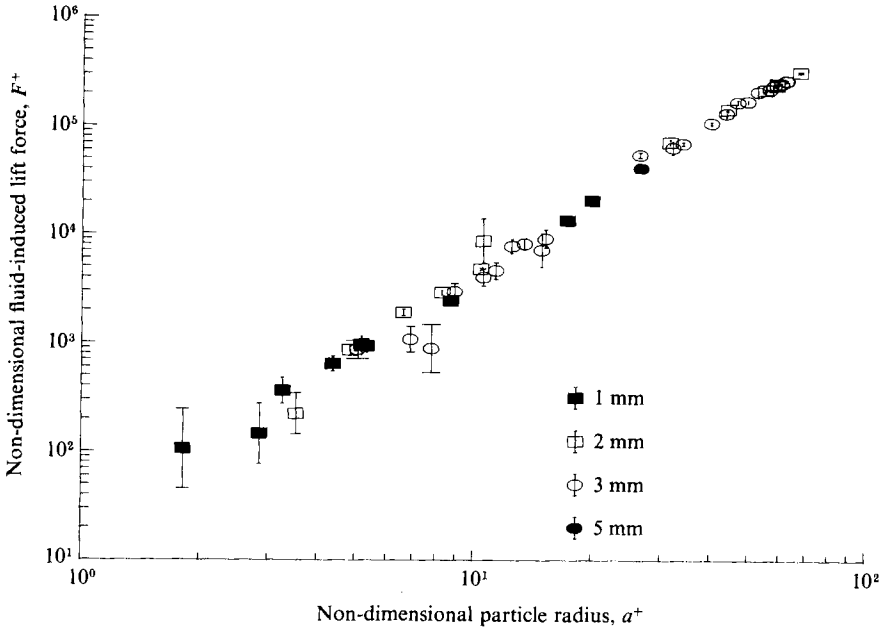

FIGURE 9. Lift force on particles on a smooth surface for various particle diameters (68% confidence limits).

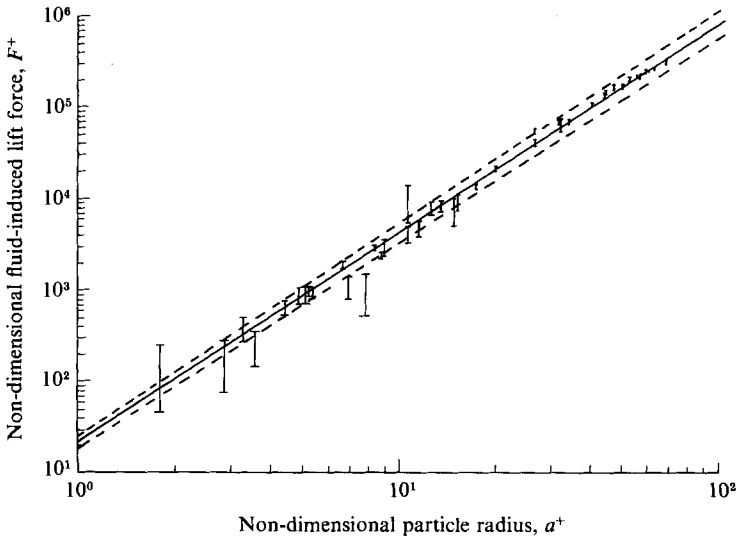

FIGURE 10. A comparison of the corrected data (68% confidence limits) with the fitted relationship for the variation of F^+ with a^+ for a particle on a smooth surface $F^+ = (20.90 \pm 1.57)\,(a^+)^{(2.31 \pm 0.02)}$, ——, best estimate, – – – 95% confidence limits.

therefore, considering the circumstances, that all four suspect points were due to instrumentation problems. (Note that the suspect points are not displayed on figure 9.)

A weighted least-squares fit on the logs of the non-suspect data gave

$$F^+ = (20.90 \pm 1.57)\,(a^+)^{(2.31 \pm 0.02)}$$

This relationship is compared with the data in figure 10.

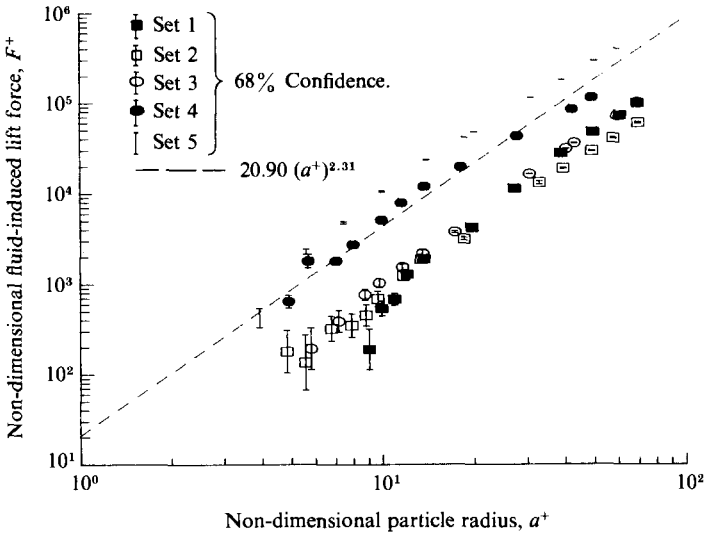

FIGURE 11. Lift forces on particles on a rough surface: log–log plot.

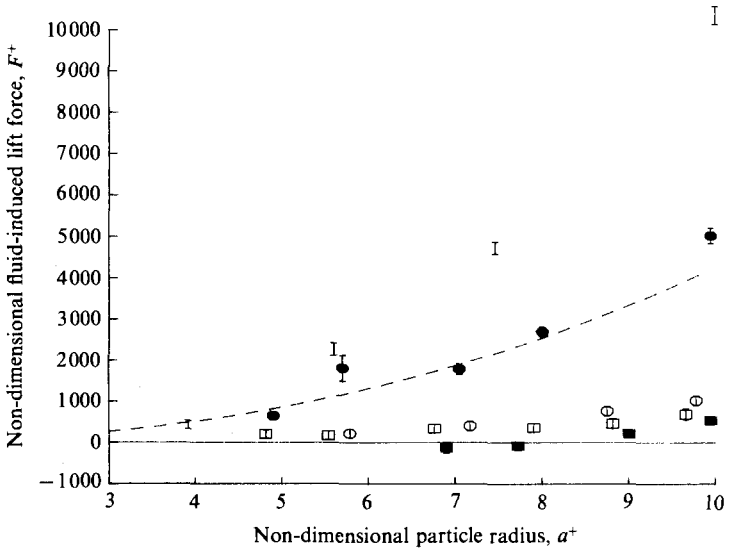

FIGURE 12. Lift forces on particles on a rough surface: linear plot. Symbols as figure 11.

5.4. *The effects of surface roughness upon* F^+

The results for the five roughness geometries displayed in figure 3 are given in figures 11 and 12. Figure 11 displays the data on a log–log plot. Figure 12 displays the data for $a^+ < 10$ on a linear plot. Note that the two points indistinguishable from zero on figure 12 are not shown on figure 11.

Figures 11 and 12 show how surface roughness can significantly change the mean fluid-induced lift forces acting on particles on surfaces, reducing the force when the particle is deposited between roughness elements (sets 1–3) and increasing it when the particle is on top of a single rod (sets 4 and 5). It is notable that the data in set

4 differ little from the smooth-surface relationship; set 5 is about double the smooth-surface values; and that sets 1–3 are about a factor of six less than the smooth-surface data.

6. Discussion

As mentioned in §1, there is no theory, valid for sphere in the sublayer region, suitable to predict the lift forces acting on particles on or near to surfaces. However, it is interesting to consider the validity of expressions that have been used to make such predictions.

Saffman (1965) derived the following expression for the lift force acting upon a sphere in a shear flow:

$$F = \frac{6.64\,\nu\,\rho\,a^2\,v\,\kappa^{\frac{1}{2}}}{\nu^{\frac{1}{2}}} \tag{1}$$

where v is the velocity difference between the particle and the fluid surrounding it, and κ is the velocity gradient of the fluid.

This is only theoretically valid in unbounded flows at very low Reynolds numbers. However, Halow (1973) used it (in modified form) to explain observations of particle motion at fairly large Reynolds numbers.

Equation (1) can be rewritten in terms of our non-dimensional variables as

$$F^+ = 6.46(a^+)^2\,v^+\,(\kappa^+)^{\frac{1}{2}}. \tag{2}$$

Kay & Nedderman (1974) give the variation of mean non-dimensional fluid velocity u^+ with non-dimensional height y^+ as

$$u^+ = y^+, \qquad y^+ < 5, \tag{3}$$

$$u^+ = -3.05 + 5.0 \ln y^+, \quad 5 < y^+ < 30, \tag{4}$$

$$u^+ = 5.5 + 2.5 \ln y^+, \qquad y^+ > 30. \tag{5}$$

Figure 13 compares the prediction of (2) with the measured values of F^+ for a particle on a surface. The non-dimensional velocity u^+ is taken to be the mean of the non-dimensional velocity at the top and bottom of the particle. The non-dimensional velocity gradient κ^+ is taken as the difference of the non-dimensional velocity over the top and bottom of the particle divided by its non-dimensional diameter. Clearly, the predictions do not agree with the experimental data, although the model seems to be approaching the data as a^+ is reduced, but still underestimates the data. It is interesting to note that at low a^+ ($a^+ < 20$) this expression is a factor of 1.7 lower than the data. This is the same as the factor by which O'Neill (1968) calculated the drag force to increase owing to the presence of the surface. However, we cannot use the above calculational procedure to estimate the variation of lift force with height, as the lift force is predicted to increase with increasing height, contrary to the experimental results. For example, as shown in figure 7, the value of F^+ decreases by a factor of 0.31 when the particle moves 250 μm away from the surface, while (2) predicts a factor of 1.09 increase.

Similarly, in figure 6, the experimental data shows that F^+ decreases as the particle height increases, in variance to the prediction based on Saffman's model. In this case, the discrepancy between the measured data and the values given by the relationship based on Saffman's expression is much less than at the higher value of a^+ and is shown on figure 6.

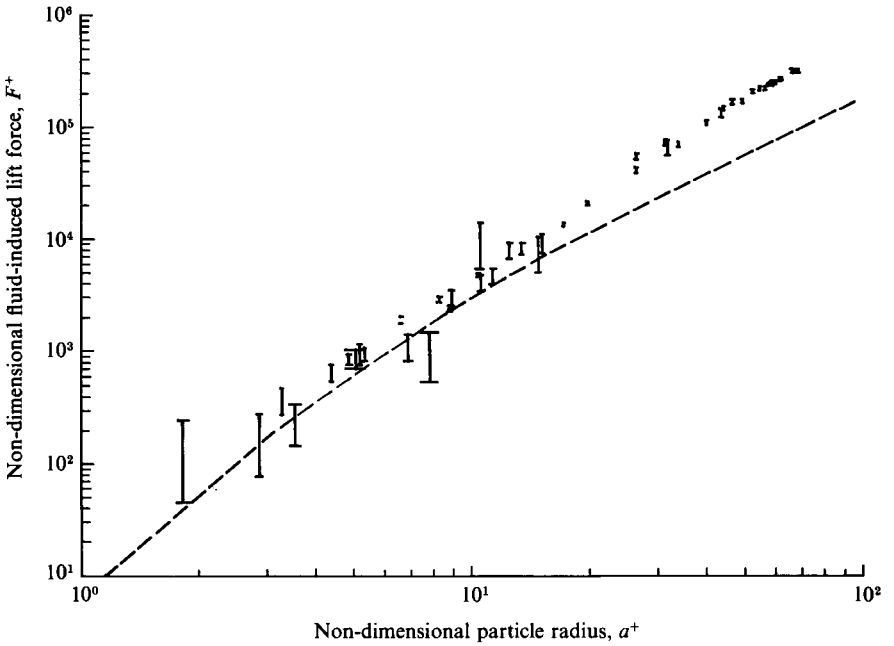

FIGURE 13. A comparison of the smooth-surface data (68% confidence limits) with the 'theoretical' predictions of Saffman (1965) (– – –).

Saffman's relationship, derived for unbounded shear flow, is frequently extrapolated to the prediction of the lift force acting on a sphere on or near to a surface. These experiments show such an extrapolation to be inappropriate.

It is interesting to note (from figure 11) that at $a^+ = 4$, the increase in lift due to the particle projecting into the higher velocity flow is no longer significant. However, the resolution of the system is insufficient to investigate the region ($a^+ < 4$) more fully.

7. Conclusions

The data recorded here ($1.8 > a^+ > 70$) for the mean fluid lift force on a sphere on a smooth surface are in good agreement with the relationship

$$F^+ = (20.90 \pm 1.57)\,(a^+)^{(2.31 \pm 0.02)}.$$

Hitherto, the most frequently used method of calculating lift forces has been based on an expression of Saffman's (1965). The work described here has shown such expressions to underpredict the data below a^+ of 20 by a factor of about 1.7 and up to a factor of 3 at higher values of a^+. In addition the lift force was found to decrease as the particle/surface gap increased in contrast to predictions made using Saffman's expression, which predicts an increase in lift force with an increase in height.

Surface roughness can significantly change the mean fluid-induced lift forces acting on particles on surfaces, reducing the force when a particle is deposited between roughness elements and increasing it when a particle is on top of a single rod. Increases of a factor of 2 and decreases of a factor of 6 in lift forces have been observed.

The only geometry where little change in lift force from that on a smooth surface is observed is when the particle is on top of one of an array of rods.

The work was carried out at the Berkeley Nuclear Laboratories of the Technology Planning and Research Division of the Central Electricity Generating Board. The paper is published with the permission of the Central Electricity Generating Board.

REFERENCES

Bretherton, F. P. 1962 *J. Fluid Mech.* **14**, 284–304.

British Standard 1042: Part 2A 1973 *Method for the Measurement of Fluid Flow in Pipes.* London: British Standards Institution.

Cleaver, J. W. & Yates, B. 1973 *J. Colloid Interface Sci.* **44**, 464–474.

Goren, S. L. 1970 *J. Fluid Mech.* **41**, 619–625.

Hall, D. 1982 *CEGB Rep.* TPRD/B/0102/N82.

Hall, D. 1984 *CEGB Rep.* TPRD/B/0516/N84.

Halow, J. S. 1973 *Chem. Engng Sci.* **28**, 1–12.

Kay, J. M. & Nedderman, R. M. 1974 *Fluid Mechanics and Heat Transfer*, 3rd edn, p. 186. Cambridge University Press.

Leighton, D. & Acrivos, A. 1985 *Z. Angew. Math. Phys.* **36**, 174–178.

O'Neill, M. E. 1968 *Chem. Engng Sci.* **23**, 1293–1298.

Pirie, M. A. M. 1978 *CEGB Rep.* RD/B/N4227.

Reeks, M. W., Reed, J. & Hall, D. 1987 On the resuspension of small particles by a turbulent flow. *J. Phys. D* (accepted for publication).

Saffman, P. G. 1965 *J. Fluid Mech.* **22**, 385–400 (and Corrigendum **31**, 1968, 624).

Willetts, B. B. & Murray, C. G. 1981 *J. Fluid Mech.* **105**, 487–505.